

# A Calculation Model of Grout Migration Height for Post-Grouting Technology

Sheng-Gen Huang <sup>1</sup>, Tao Zhang <sup>1,\*</sup> and Hui Cao <sup>2</sup><sup>1</sup> Faculty of Engineering, China University of Geosciences, Wuhan 430074, China; huangshgr@163.com<sup>2</sup> The School of Foreign Languages, China University of Geosciences, Wuhan 430074, China; caohg@163.com

\* Correspondence: zhangtao@cug.edu.cn

**Abstract:** Post-grouting technology has been extensively used in geotechnical engineering to improve the bearing capacity of various piles, which overcomes the technical limitations of the bored piles and recovers the mechanical performance of strata. A considerable amount of earlier research has been conducted to investigate the bearing behavior and reinforcement mechanism of the grouted piles, while very few studies focus on the reinforcement area of post-grouting technique. The theoretical analysis on reinforcement area is of great significance, which is beneficial to correlate the grouting parameters with pile bearing capacity with a target of saving cost and acquiring an optimized design. This paper conducted a theoretical analysis on the grout migration height, and then proposed a new predictive model to estimate the ultimate migration height of cement slurry, where the grout rising process is considered as the flow of Bingham fluid in an axial annular space. A field test was conducted to verify the applicability of the proposed model, and the comparison results revealed that the calculated height is slightly overestimated as compared to the actual values, but it is acceptable in engineering design. The grouting pressure loss and induced permeation was warranted to be studied in future.

**Keywords:** bored piles; post-grouting; slurry migration height; theoretical model



**Citation:** Huang, S.-G.; Zhang, T.; Cao, H. A Calculation Model of Grout Migration Height for Post-Grouting Technology. *Appl. Sci.* **2022**, *12*, 6327. <https://doi.org/10.3390/app12136327>

Academic Editor: Tiago Miranda

Received: 31 May 2022

Accepted: 20 June 2022

Published: 21 June 2022

**Publisher's Note:** MDPI stays neutral with regard to jurisdictional claims in published maps and institutional affiliations.



**Copyright:** © 2022 by the authors. Licensee MDPI, Basel, Switzerland. This article is an open access article distributed under the terms and conditions of the Creative Commons Attribution (CC BY) license (<https://creativecommons.org/licenses/by/4.0/>).

## 1. Introduction

Bored pile, due to the strong adaptability to different formation conditions, high bearing capacity, and flexibly geometry size, has been widely employed in geotechnical engineering applications around the world [1–5]. However, two technological limitations of the bored pile with respect to the sediment presence at pile base and weak soil layers around the pile shaft, greatly reduce the ultimate bearing capacity of the pile, and then increase the pile settlement [6]. The post-grouting technology has been demonstrated to overcome these two limitations. Furthermore, the bearing capacity and reliability of the bored piles could be improved after the grouting process [7–10]. For the post-grouting technology, the U-tube grouting system composed of an inlet pipe, an outlet pipe, and a pile base grouting device is designed to inject solidifiable cement slurry into both the base and sides of pile, resulting in a mechanical improvement of loose sediments at pile base and a soil solidification around pile shaft by resorting to filling, permeating, replacing, splitting, compacting, consolidating, and so forth [11–15]. Thus, this advanced technology has attracted great attention from geotechnical engineers and designers.

Many previous field experiments have been conducted to investigate the influences of post-grouting on the bearing behavior of bored piles [16–18]. Bruce [19] clearly revealed the benefits of post-grouting to enhance the service performance of large diameter piles. Stocker [20] had made a comprehensive and quantitative field loading test, where the skin friction of cast-in-situ bored piles with post-grouting at a settlement of 20 mm was reported to have an increment of 100–120% compared with that of the ungrouted piles. Gouvenot and Gabiax [21] conducted the field tests to evaluate the bearing capacity of

post-grouted piles in sand and clay layers. It is reported that the ultimate bearing capacity is found to be increased by 200–300%, which could greatly reduce the construction cost and create a huge economic benefit. Huang and Gong [22] had conducted the back analysis on the post-grouting piles, in which the deformation modulus and the average frictional resistance of soil along the shaft, respectively, increase by 33–67% and 30–40% after the post-grouting treatment. Dai et al. [8] measured the bearing capacities of bored pile at Suramadu Bridge before and after grouting. They reported that the side frictional resistance, the pile-base resistance, and the ultimate bearing capacity of the investigated pile, respectively, increase by 9–30%, 34–45%, and 17–62%. Skiwinski and Flemming [23] found that the post-grouting obviously reduced the downward displacement of bored piles as compared to the counterpart under the same loading conditions. These previous studies have demonstrated that the post-grouting technology possesses excellent performance of improving the bearing behavior of bored piles and the stability of superstructures. However, a clear understanding of the reinforcement mechanism of post-grouting technology has not been achieved presently. Pouranapillai et al. [24] indicated that the plastic deformation of the soils around pile can be eliminated due to the pre-loading effect. In other words, an intact bulb is generated as a result of the compaction effect of post-grouting, which enlarges the bearing area compared with the shaft area at the tip. This pile bearing capacity improvement is mainly attributed to two facts: (i) the injected cement slurry solidifies the weak soil layers and losses sediments around and at the bottom of pile, respectively; (ii) the expansion of cement slurry at pile base increases the bearing area, resulting in an enhancement of pile-base resistance, and the slurry migration along the pile equals to make an increment in pile diameter. However, very little research has comprehensively addressed the intrinsic correlation of pile bearing capacity with post-grouting design parameters, especially for the migration height of slurry.

This paper aimed to develop a theoretical model of grout migration height for the post-grouting technology. The rheological equation of Bingham fluid was employed to describe the upward migration of cement slurry along the pile shaft. Two field loading tests were conducted on the post-grouted piles of the Duxiapu bridge and Henan development plaza in China to verify the applicability of the obtained model. It is believed that this proposed theoretical model is useful to optimize the engineering design of post-grouted piles.

## 2. Solution of Grout Migration Height

### 2.1. Basic Assumptions

The real behavior of upward migration of cement slurry in the weak layer zone is too sophisticated to be analyzed. Therefore, the post-pile foundation (as shown in Figure 1) is simplified and simulated by a cylindrical model consisting of bored pile, weak layer zone, and surrounding soil, in which  $L$  is the length of bored pile, and  $r_0$  and  $b$  the radius of bored pile and the thickness of weak layer, respectively. The following assumptions are employed for making the theoretical solution of the grout migration height in this study:

- (i) soils around the bored pile are isotropic and homogeneous;
- (ii) cement slurry is simplified as the incompressible, isotropic and homogeneous Bingham fluid;
- (iii) surface of bored pile and hole is considered as cylindrical surface, and the annular cement slurry is homogeneously distributed.

It should be acknowledged that the Herschel-Bulkley model is superior as compared to Bingham model in the calculation of grout migration height. Meanwhile, the Bingham model is much easier and the required calculation parameters are easily be obtained. Therefore, the Bingham model is selected in this manuscript for developing the calculation model of migration height.

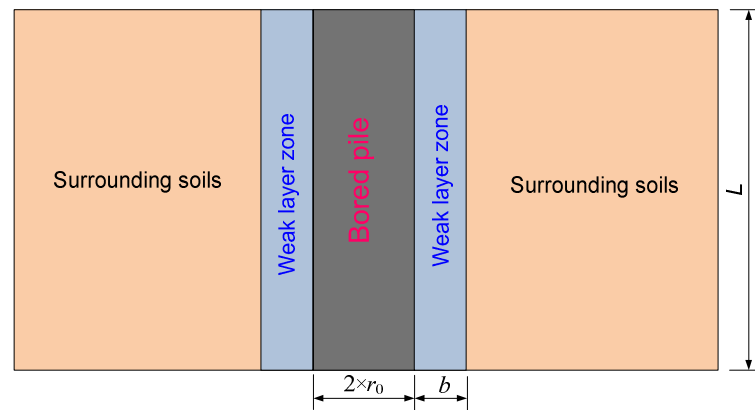


**Figure 1.** Calculation model of the post-grouted pile foundation.

## 2.2. Governing Equation

Figure 2 shows the strained condition of grout in an annular space, where a small annular cement slurry element of size  $dr$  by  $dz$  is selected. The cement slurry is considered as a steady flow, and thus, the component of Newton's second law along the pile length direction,  $z$ , can be written as:

$$\sum dF_z = 2\pi r dr \cdot p + 2\pi r dz \cdot \tau_z - 2\pi(r + dr) \cdot \left( \tau_z + \frac{d\tau_z}{dr} dr \right) dz - 2\pi r dr \left( p + \frac{dp}{dz} dz \right) - 2\pi r dr dz \cdot \rho_c g \quad (1)$$

where  $\sum dF_z$  is the sum of the  $z$  components of all forces acting on the small annular cement slurry element, which has mass  $dm = 2\pi r dr dz \rho_c$ ;  $p$  is the pressure at the bottom surface of annular element;  $\tau_z$  is the shear stress along the pile length direction; and  $\rho_c$  is the cement slurry density.

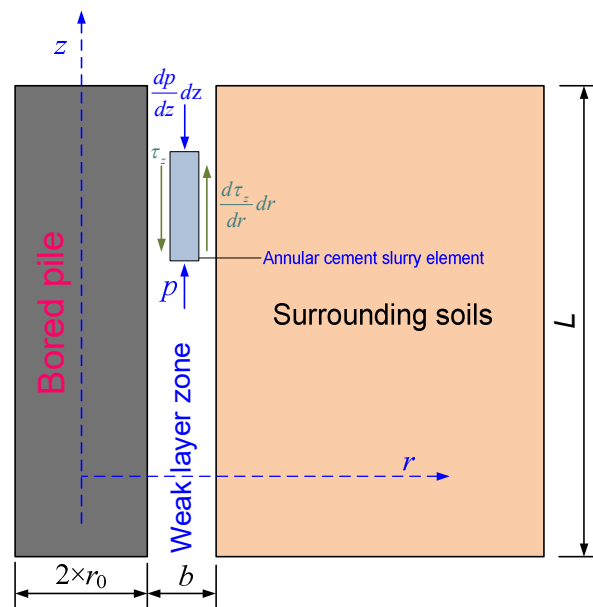


**Figure 2.** Strained condition of grout in an annular space.

Let  $\sum dF_z = 0$ , ignore third order infinitesimal, Equation (1) can be rearranged as:

$$\frac{dp}{dz} + \frac{1}{r} \tau_z + \frac{d\tau_z}{dr} + \rho_c g = 0 \quad (2)$$

The rheological equation of Bingham fluid can be expressed as:

$$\tau = \tau_0 + \eta \frac{dv}{dr} \quad (3)$$

where  $v$  is the shear rate; and  $\tau_0$  is the yield shear strength (Pa). By integrating Equation (2) with respect to  $r$ , the following equation can be obtained:

$$\tau = -\frac{r}{2} \left( \frac{dp}{dz} + \rho_c g \right) + \frac{c_1}{r} \quad (4)$$

Then, the boundary conditions can be written as follows:

$$\tau|_{r=r_0+b/2} = 0 \quad (5)$$

$$v|_{r=r_0} = 0 \quad (6)$$

$$v|_{r=r_0+b} = 0 \quad (7)$$

By means of (5) and suitable manipulation, Equation (4) can be rewritten as:

$$\tau = c_1 \left[ \frac{1}{r} - \frac{r}{(r_0 + b/2)^2} \right] \quad (8)$$

Substituting Equation (4) to (5) yields:

$$c_1 = \frac{1}{2} \left( r_0 + \frac{b}{2} \right)^2 \left( \frac{dp}{dz} + \rho_c g \right) \quad (9)$$

The radius ratio of the weak layer zone to the bored pile can be described as  $R_H = \frac{b}{r_0}$ . By means of Equations (6) and (7), then Substituting Equation (8) into Equation (3) gives:

$$c_1 = \frac{\tau_0 R_H}{\ln(1 + R_H) - \frac{2R_H}{2+R_H}} \quad (10)$$

Change the form of Equation (9):

$$\frac{dp}{dz} = \frac{2c_1}{\left( r_0 + \frac{b}{2} \right)^2} - \gamma_c \quad (11)$$

where  $\gamma_c$  is the unit weight of cement slurry ( $\text{kN/m}^3$ ),  $\gamma_c = \rho_c g$ .

Defining  $m = \frac{2c_1}{\left( r_0 + \frac{b}{2} \right)^2} - \gamma_c$  and integrating Equation (10) with respect to  $z$ , the following relationship is obtained:

$$p = mz + p_0 \quad (12)$$

where  $p_0$  is the grouting outlet pressure (kPa); and  $p$  is the pressure of cement slurry at depth of  $z$  (kPa). The start-crack pressure  $p_c$  at depth of  $z$  can be expressed as:

$$p_c = k_0 \cdot \gamma \cdot (H - z) + \sigma_{cl} \quad (13)$$

where  $k_0$  denotes lateral earth pressure coefficient of soil around bored pile;  $\gamma$  is the unit weight of soil ( $\text{kN/m}^3$ );  $H$  is the depth of grouting outlet point in ground;  $z$  is the migration height of cement slurry;  $\sigma_{cl}$  is the tensile stress of the two weak interfaces (kPa).

According to the results reported by Zhang et al. [25], tensile stress value of weak interfaces is very small and can be omitted in this study, so the start-crack pressure can be simplified as follow:

$$p_c = k_0 \cdot \gamma \cdot (H - z) \quad (14)$$

The crack in the weak layer around the pile don't stop generating until the start-crack pressure greater or equal to pressure of cement slurry at depth of  $z$ , it can be expressed as:

$$p_c(z) = p(z) \quad (15)$$

The radius ratio of the weak layer zone to the bored pile can be described as  $R_h = \frac{b}{h_0}$ , substituting Equations (12) and (14) into Equation (15), the maximum migration height of cement slurry can be derived as:

$$z = \frac{k_0 \gamma H - p_0}{m + k_0 \gamma} \quad (16)$$

Due to the friction and collision of particle in the cement slurry during the process of grouting, the outlet pressure  $p_0$  is smaller than the gage pressure, which can be expressed as follow:

$$p_0 = p_1 + p_2 - \Delta p \quad (17)$$

where  $p_1$  is gage pressure;  $p_2$  is static pressure of grout; and  $\Delta p$  represents pressure loss. According to the earlier research conducted by Dai et al. (2018), the relationship between pressure loss  $\Delta p$  and pipe length  $L$  can be expressed as:

$$\Delta p = 0.037L \quad (18)$$

Substituting Equations (17) and (18) into Equation (16), the solution of cement slurry migration height would be obtained.

### 3. Results and Discussion

#### 3.1. Parameter Influence Analysis

The parameter influence analysis was carried out to explore the correlations of slurry migration height with the input parameters. It is assumed that the surrounding soil is isotropic and homogeneous, the unit weight of soil is  $\gamma = 18 \text{ kN}$ , and the yield shear strength of cement slurry is  $\tau_0 = 6 \text{ Pa} \cdot \text{s}$ . A total of 15 samples with different geometric conditions were selected and classified into three sets, as listed in Table 1. The influencing factors include pile length, pile radius, and thickness of weak layer in the following section.

**Table 1.** Grouting pressure, pile radius, and grouting depth of 15 samples for calculation.

Set	Grouting Pressure/kPa	Pile Radius/m	Grouting Depth/m
1	different value	0.4	20
2	1500	different value	20
3	1500	0.4	different value

Figure 3a presents the relationship between pile embedment depth and migration height. A linear decreasing trend was observed for these two parameters, in which migration height decreases with an increase in pile embedment depth. It can be deduced that for the bored pile with short length, its bearing capacity is more sensitive to the treatment of post-grouting. The correlation of migration height with pile diameter is shown in Figure 3b, where migration height increases with the increasing of pile diameter, and this increment of height becomes moderate as the pile diameter exceeds 1.0 m. This phenomenon reveals that the migration height would be a stable value as pile diameter further increased. For the bored piles with large diameters, the discrepancy of migration height is expected to be insignificant for the same post-grouting technology. The relationship of migration height with grouting pressure is presented in Figure 3c. It can be expected that a higher grouting pressure would result in a larger migration height as shown in figure. The high value of grouting pressure imposes the strict requirements on the grouting equipment and construction cost. In the actual grouting construction of cast-in-place pile, due to the complexity of the geological conditions and difference in pile length and mud thickness, the actual

migration height values of cement slurry in piles are different from each other. Thus, the actual cement slurry migration height should be determined in situ.

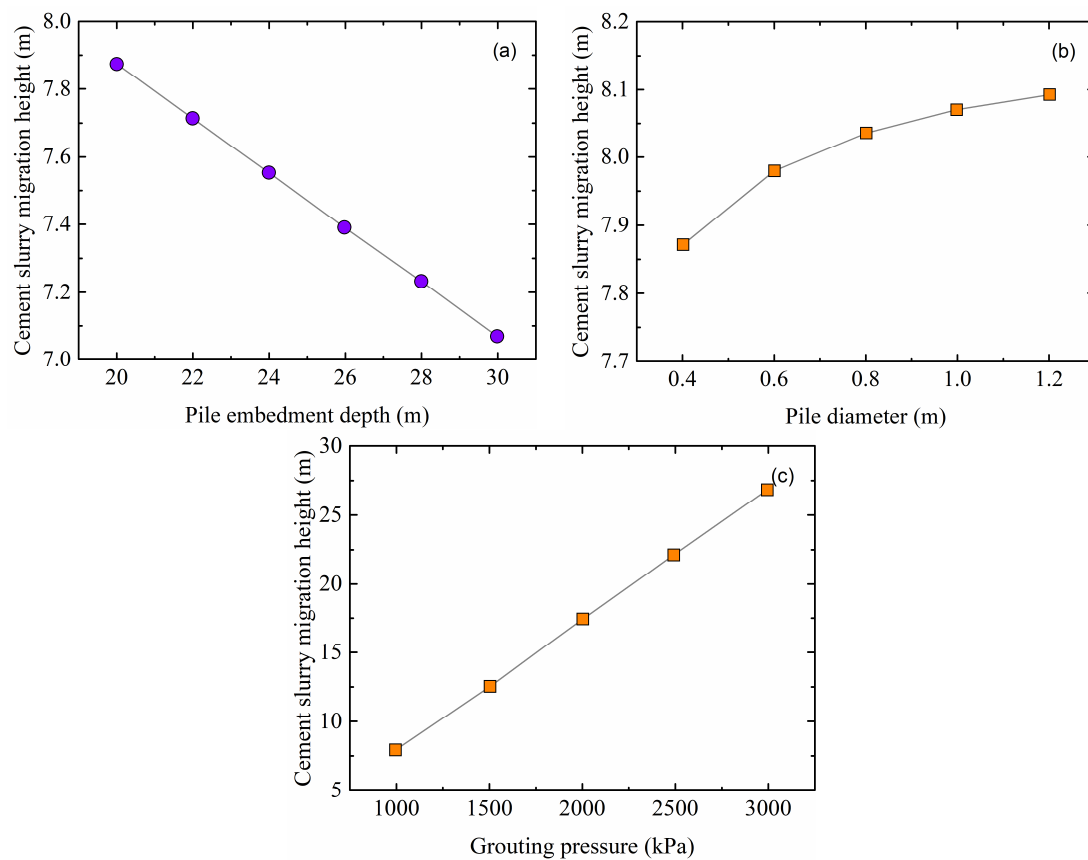


**Figure 3.** Correlations of cement slurry migration height with: (a) pile embedment depth; (b) pile diameter; and (c) grouting pressure.

### 3.2. Model Validation

To verify the obtained solution of slurry migration height, a field test at the Duxiapu bridge, Zhejiang province, China was conducted. The post-grouted method is adopted to improve the bearing capacity of bored piles in this project. The geological parameters of test pile and layout of grouting pipes are shown in Figure 4. The Silty clay serves as the bearing stratum for the bored piles. The pile is 42.5 m in length and 800 mm in diameter. Both base and shaft grouting are adopted to reinforce the bored piles at the same time, where the shaft grouting point locates in the medium sand. A total of 3 tons of cement slurry with cement ratio of 0.5 were consumed, of which 1 ton is for shaft grouting and the rest 2 tons are for base grouting. The grouting pressure was set as 2.0 MPa in this application. After 30 days curing, the foundation pit was excavated at a depth of 14 m. During the excavation process, the detailed information of the solidified cement slurry on 5 piles were clearly obtained. The firstly observed depth values of solidified cement slurry are shown in Table 2. According to these measured depth values, the slurry migration height can be easily calculated by subtracting from the depth of shaft grouting outlet (21.5 m in this study). Therefore, the actual migration height ranges from 10.69 m to 11.44 m for these five piles.



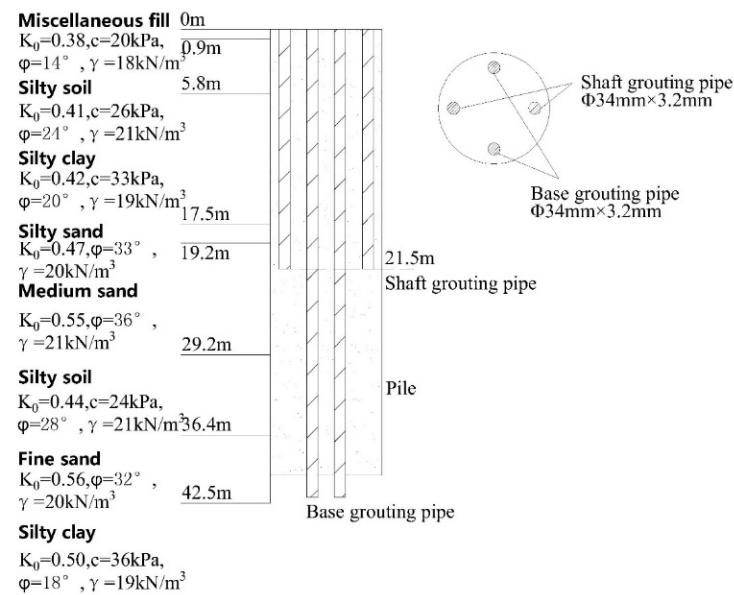


**Figure 4.** Formation of construction site and layout of grouting pipes.

**Table 2.** First observed depth of cement slurry for 5 bored piles.

Pile Number	Observed Depth (m)	Actual Migration Height (m)
1	10.06	11.44
2	10.58	10.92
3	10.36	11.14
4	11.23	10.27
5	10.81	10.69

Figure 5 shows the photos of observed solidified cement slurry on piles, where the actual rising height of grouting varies in different directions. Based on the field conditions motioned above, the pile radius is  $r_0 = 0.4$  m, depth of shaft grouting outlet is  $H = 21.5$  m, unit weight of grout is  $\gamma_c = 18$  kN/m<sup>3</sup>, and gage pressure of shaft grouting is  $p_1 = 1.8$  MPa. Since the lateral earth pressure coefficient and unit weight of each soil layer are different, the weighted average method is employed in the calculation. The weighted average lateral earth pressure coefficient is  $k_0 = 0.43$ , and the weighted average unit weight of soil is  $\gamma = 19.65$  kN/m<sup>3</sup>. In addition, five grout samples were tested in the laboratory, and the yield shear strength of cement slurry is determined as  $\tau_0 = 6$  Pa. The average thickness of weak layer measured on 5 piles is  $b = 0.05$  m.

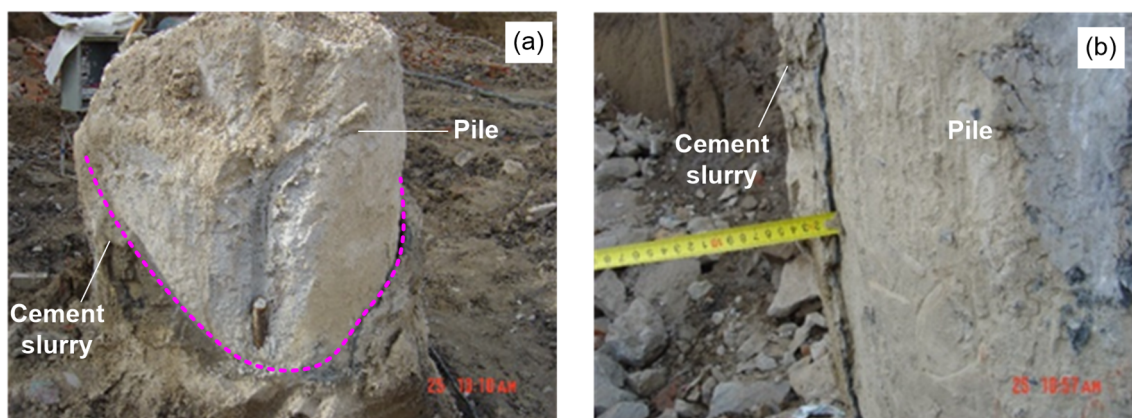


**Figure 5.** Photos of the bored pile after excavation: (a) solidified cement slurry and (b) thickness measurement.

According to the Equations (17) and (18), the outlet pressure  $p_0$  can be calculated:

$$p_0 = p_1 + p_2 - \Delta p = 1800 + 21.5 \times 19.65 - 0.037 \times 21.5 = 1427 \text{ kPa}$$

Parameter  $c_1$  can be derived by Equation (10):

$$c_1 = \frac{\tau_0 R_H}{\ln(1 + R_H) - \frac{2R_H}{2+R_H}} = \frac{-0.006 \times 0.075}{\ln(1+0.075) - \frac{2 \times 0.075}{2+0.075}} = -8.3 \text{ kPa} \cdot \text{m}$$

Then parameter  $m$  can be derived by:

$$m = \frac{2c_1}{\left(r_0 + \frac{b}{2}\right)^2} - \gamma_c = \frac{2 \times -8.3}{\left(0.4 + \frac{0.03}{2}\right)^2} - 19.65 = -114 \text{ kN/m}^3$$

Finally, the migration height of cement slurry can be obtained by Equation (16):

$$z = \frac{p_0 - k_0 \gamma H}{-m - k_0 \gamma} = \frac{1427 - 0.43 \times 19.65 \times 21.5}{84.3 - 0.43 \times 19.65} = 11.90 \text{ m}$$

Compared with the actual migration height of 10.69 m~11.44 m, the calculated value of 11.90 m is slightly overestimated but fully acceptable from a viewpoint of engineering design. This overestimation is mainly attributed to the combined impacts of grouting pressure loss and cement slurry permeation during the post-grouting process.

#### 4. Conclusions

Studying the reinforcement scope of post-grouting is of great significance. It contributes to create a bridge to connect the pile bearing capacity with grouting parameters, which makes post-grouting design more reasonable and economic. A theoretical analysis on migration height of grouting slurry is conducted in this paper. The rising process of slurry is simplified as the flow of Bingham fluid in an axial annular space. After that, a useful formula is developed to estimate the migration height value. The parameter influence analyses show that the investigated migration height is closely related to the pile embedment depth, pile diameter, and grouting pressure.

In order to verify the proposed calculation model, five bored piles treated with post-grouting technology were selected and excavated after treatment to obtain the actual migration height. The comparison results indicated that the calculated height from proposed model is slightly smaller than the actual values, while it is fully acceptable in engineering design. It is noteworthy that the pressure loss and the resulted permeation during grouting process also have important influence on the slurry migration, which is recommended to be further investigated in future.

**Author Contributions:** Conceptualization, validation, and writing—review and editing, S.-G.H.; methodology, T.Z.; writing—review and editing, H.C. All authors have read and agreed to the published version of the manuscript.

**Funding:** This research received no external funding.

**Institutional Review Board Statement:** Not applicable.

**Informed Consent Statement:** Not applicable.

**Data Availability Statement:** Not applicable.

**Acknowledgments:** Thank you for the helps provided from the editor and the reviewers to improve this paper.

**Conflicts of Interest:** The authors declare no conflict of interest.



## References

1. Touma, F.T.; Reese, L.C. Behavior of bored piles in sand. *J. Geotech. Eng. Div.* **1974**, *100*, 749–761. [\[CrossRef\]](#)
2. Tsuji, M.; Kobayashi, S.; Mikake, S.; Sato, T.; Matsui, H. Post-grouting experiences for reducing groundwater inflow at 500 m depth of the Mizunami underground research laboratory, Japan. *Procedia Eng.* **2017**, *191*, 543–550. [\[CrossRef\]](#)
3. Ye, X.; Wang, S.; Zhang, S.; Xiao, X.; Xu, F. The compaction effect on the performance of a compaction-grouted soil nail in sand. *Acta Geotech.* **2020**, *15*, 2983–2995. [\[CrossRef\]](#)
4. Cui, Y.L.; Qi, C.G.; Zheng, J.H.; Wang, X.Q.; Zhang, S.M. Field test research on post-grouting effect for super-long cast-in-place bored pile in thick soft foundation. *Geotech. Geol. Eng.* **2021**, *39*, 4833–4842. [\[CrossRef\]](#)
5. Zhang, Q.Q.; Li, H.T.; Cui, W.; Zhao, Y.H.; Wang, S.L.; Xu, F. Analysis of Grout Diffusion of Postgrouting Pile Considering the Time-Dependent Behavior of Grout Viscosity. *Int. J. Geomech.* **2021**, *21*, 04021201. [\[CrossRef\]](#)
6. Ng, C.W.; Yau, T.L.; Li, J.H.; Tang, W.H. New failure load criterion for large diameter bored piles in weathered geomaterials. *J. Geotech. Geoenvironmental Eng.* **2001**, *127*, 488–498. [\[CrossRef\]](#)
7. Wang, Z.F.; Shen, S.L.; Ho, C.E.; Kim, Y.H. Investigation of field-installation effects of horizontal twin-jet grouting in Shanghai soft soil deposits. *Can. Geotech. J.* **2013**, *50*, 288–297. [\[CrossRef\]](#)
8. Dai, G.; Gong, W.; Zhao, X.; Zhou, X. Static testing of pile-base post-grouting piles of the Suramadu bridge. *Geotech. Test. J.* **2011**, *34*, 34–49.
9. Wan, Z.H.; Dai, G.L.; Gong, W.M. Study on the response of postside-grouted piles subjected to lateral loading in calcareous sand. *Acta Geotech.* **2021**, 1–17. [\[CrossRef\]](#)
10. Zhou, Z.; Wang, K.; Feng, H.; Tian, Y.; Zhu, S. Centrifugal model test of post-grouting pile group in loess area. *Soil Dyn. Earthq. Eng.* **2021**, *151*, 106985. [\[CrossRef\]](#)
11. Bolton, M.D.; McKinley, J.D. Geotechnical properties of fresh cement grout—pressure filtration and consolidation tests. *Géotechnique* **1997**, *47*, 347–352. [\[CrossRef\]](#)
12. Shen, S.L.; Han, J.; Du, Y.J. Deep mixing induced property changes in surrounding sensitive marine clays. *J. Geotech. Geoenvironmental Eng.* **2008**, *134*, 845–854. [\[CrossRef\]](#)
13. Shen, S.L.; Wang, Z.F.; Horpibulsuk, S.; Kim, Y.H. Jet grouting with a newly developed technology: The twin-jet method. *Eng. Geol.* **2013**, *152*, 87–95. [\[CrossRef\]](#)
14. Shen, S.L.; Wang, Z.F.; Yang, J.; Ho, C.E. Generalized approach for prediction of jet grout column diameter. *J. Geotech. Geoenvironmental Eng.* **2013**, *139*, 2060–2069. [\[CrossRef\]](#)
15. Shen, S.L.; Wang, Z.F.; Cheng, W.C. Estimation of lateral displacement induced by jet grouting in clayey soils. *Géotechnique* **2017**, *67*, 621–630. [\[CrossRef\]](#)
16. Lin, C.; Han, J.; Shen, S.; Hong, Z. Numerical modeling of laterally loaded pile groups in soft clay improved by jet grouting. In Proceedings of the Grouting and Deep Mixing, New Orleans, LA, USA, 15–18 February 2012; pp. 2052–2060.
17. Zhang, N.; Shen, J.S.; Zhou, A.; Arulrajah, A. Tunneling induced geohazards in mylonitic rock faults with rich groundwater: A case study in Guangzhou. *Tunn. Undergr. Space Technol.* **2018**, *74*, 262–272. [\[CrossRef\]](#)
18. Zhang, N.; Shen, J.S.; Lin, C.; Arulrajah, A.; Chai, J.C. Investigation of a large ground collapse and countermeasures during mountain tunnelling in Hangzhou: A case study. *Bull. Eng. Geol. Environ.* **2019**, *78*, 991–1003. [\[CrossRef\]](#)
19. Bruce, D.A. Enhancing the performance of large diameter piles by grouting. *Ground Eng.* **1986**, *19*, 9–15.
20. Stocker, M. The influence of post grouting on the load bearing capacity of bored piles. In Proceedings of the 8th European Conference on Soil Mechanics and Foundation Engineering, Helsinki, Finland, 23–26 May 1983; Volume V1, pp. 167–170.
21. Gouvenot, D.; Gabiix, F.D. A new foundation technique using piles sealed by concrete under high pressure. In Proceedings of the 7th Annual Offshore Technical Conference, Houston, TX, USA, 4–7 May 1975.
22. Huang, S.G.; Gong, W.M. Study on bearing behavior of super long-large diameter piles after grouting. *Chin. J. Geotech. Eng.* **2006**, *1*, 113–117.
23. Silwinski, Z.J.; Flemming, W.G.K. The integrity and performance of bored piles. In Proceedings of the International Conference on Advances in Piling and Ground Treatment for Foundations, London, UK, 2–4 March 1984.
24. Pooranampillai, S.; Elfass, S.; Vanderpool, W.; Norris, G. The effects of compaction post grouting of model shaft tips in fine sand at differing relative densities-experimental results. In *Art of Foundation Engineering Practice*; Geo-Institute/American Society of Civil Engineers: Reston, VA, USA, 2010; pp. 486–500.
25. Zhang, Z.M.; Zhang, G.X.; Wu, Q.Y. Studies on characteristics of mudcake and soil between bored piles. *Chin. J. Geotech. Eng.* **2006**, *28*, 695–699.